Peer-reviewed version available at *Life* **2019**, *9*, 79; doi:10.3390/life9040079

Article

Atmospheric Nitrate as a Potential Nutrient for Life on Mars

Jianxun Shen [1,*], Aubrey L. Zerkle [1], Eva Stueeken [1] and Mark W. Claire [1]

[1] School of Earth and Environmental Sciences and Centre for Exoplanet Science, University of St Andrews, St Andrews KY16 9AL, Scotland, UK

* Correspondence: js365@st-andrews.ac.uk

Abstract: Nitrate is rich in Mars sediments owing to long-term atmospheric photolysis, oxidation, and deposition coupled with a lack of leaching via rainfall. The Atacama Desert in Chile, which is similarly dry and rich in nitrate deposits, is used as a Mars analog in this study to explore the potential effects of high nitrate levels on microbial growth. Seven study sites sampled across an aridity gradient in the Atacama Desert were categorized into 3 clusters – hyperarid, intermediate, and arid sites, as defined by major elements in the regolith, associated biomass, and precipitation. Intriguingly, the distribution of nitrate concentrations in the shallow subsurface suggests that the buildup of nitrate is not solely controlled by precipitation. Correlations of nitrate with SiO_2/Al_2O_3 and grain sizes suggest that sedimentation rates are also important in controlling nitrate distribution. At arid sites receiving more than 10 mm/yr precipitation, rainfall shows a stronger impact on biomass than nitrate does. However, high nitrate to organic carbon ratios are generally beneficial to N assimilation as evidenced both by soil geochemistry and enriched culturing experiments. This study suggests that even in the absence of precipitation on contemporary Mars, the nitrate levels are sufficiently high to benefit potentially extant Martian microorganisms.

Keywords: nitrate; Mars; Atacama Desert; sedimentation rates; biomass preservation; extremophiles

1. Introduction

Nitrogen (N) is one of the essential elements in amino acids and nucleic acids, which are fundamental building blocks for terrestrial life. Nitrogen constitutes only 2.6% of the Martian atmosphere [1], which is much lower than the 78% of nitrogen on Earth, and therefore might be considered as limiting to (past or present) Martian life [2]. Additionally, N_2 is a fairly inert molecule, and it is uncertain if other biospheres would necessarily have developed the ability to enzymatically convert it into bioavailable forms. However, nitrate salts, which form an abundant component of Martian sediments [3], could provide the dominant N source to potential Martian life.

The Atacama Desert has been used as a terrestrial Mars analog for exoplanet studies since 2003 [4] due to its extreme dryness and high UV flux. The Atacama Desert occupies around 105,000 km^2 of northern Chile, and is enclosed by two mountain rain shadows (the Coastal Cordillera and Altiplano/Andes Mountains) [5]. Due to this unique geographic location, the Humboldt current and the Pacific anticyclone [6], the Atacama has remained dry for the past 150 Myr [7] and extremely dry (with annual precipitation at the low elevation hyperarid core less than 2 mm [8]) for more than 10 Myr [9]. Within the hyperarid core, Yungay region is studied the most as a dry limit of life with the mean annual precipitation as low as 0.7 mm during typical dry years (1994-1998) [6]. In addition, both the high and low altitude Atacama Deserts are exposed to extreme surficial UV irradiation as high as ~150 kWh/m^2 in the UV-A (315–400 nm) and ~5 kWh/m^2 in the UV-B (280–315 nm), more than 40% greater than the average UV-B intensity in northern Africa [10]. UV irradiation in these bands can both destroy organic matter [11,12] and photochemically produce oxyanions such as nitrate [4,13].

Peer-reviewed version available at Life 2019, 9, 79; doi:10.3390/life9040079

Nitrate was recently detected in mudstone deposits at Gale Crater on Mars at levels of 70 to 1,100 ppm by the Mars Science Laboratory [3]. Similar nitrate levels were determined in Martian meteorites such as EETA79001 [14] and Tissint [15]. These levels are very close to nitrate levels measured in Atacama sediments during previous studies [13,16-18]. The large repositories of nitrate in the Atacama Desert are a product of atmospheric photolytic reactions, as indicated by the anomalous $\Delta^{17}O$ signals in Atacama salts [13,16]. Analogous processes are hypothesized to occur on Mars [19], although it is difficult to match the inferred NO_3/ClO_4 ratios using purely gas-phase chemistry [20]. Since rainfall is extremely limited in the Atacama Desert, atmospherically-produced salts are not solubilized as elsewhere on Earth, and can build up to very high levels [21,22]. We propose that the high levels of nitrate that build up under these hyperarid conditions could provide the dominant source of bioavailable N for local microbial communities, both in surface regolith and at depth.

Nitrate acts not only as a source of N for biomass production, but also an energy source for life in chemotrophic metabolisms. Being an oxidizing agent, nitrate is an important electron acceptor in nature [23]. Nitrate (or nitrite) can be used in chemotrophic metabolisms such as denitrification, dissimilatory reduction of nitrate to ammonium (DNRA), and anaerobic ammonium oxidation [24,25]. Therefore, beyond its universal importance in biomass production, nitrate can further stimulate the growth of microorganisms that utilize these chemotrophic metabolisms.

Previous workers have identified a wide range of microorganisms persisting in Atacama Desert soils, even within the hyperarid setting. *Actinobacteria* are generally the predominant bacterial phylum in the hyperaird core of the Atacama Desert [26-30], with most of the detected species belonging to the genus *Frankia* [26]. Other common dominant bacteria are from *Chloroflexi* [31], *Gemmatimonadetes*, *Planctomycetes* [32], *Proteobacteria*, *Firmicutes* [33], *Aquificae*, and *Deinococcus-Thermus* [28]. *Cyanobacteria*, especially those from genus *Chroococcidiopsis*, have been identified in both hypolithic [34-36] and endolithic environments [37,38]. Prokaryotic species found in the surface layer of the Atacama Desert include more irradiation-tolerant bacteria, such as *Geodermatophilaceae* and *Rubrobacter*, while more halophilic or halotolerant bacteria (e.g., *Comamonadaceae*, *Bacillaceae*, and *Alicyclobacillaceae*) and archaea (e.g., *Halobacteria*) were usually detected at depths of 20 to 100 cm [39]. Many of these taxa can perform denitrification, assimilatory and dissimilatory nitrate reduction (Kyoto Encyclopedia of Genes and Genomes, [40]). However, the activity of microbial nitrate reducers is generally inhibited when the nitrate pool increases up to thousands of parts per million [17,41], like in some regions in the Atacama Desert.

Previous studies suggest that microbial metabolic activity fluctuates episodically with relative soil humidity [39]. Because of low organic C/N ratios, the Atacama soils are assumed to be C-limited with very slow carbon cycling [42]. Microbial C mineralization remains at low levels even with enhanced moisture input. Compared to less arid regions, the microbial communities from the hyperarid core usually have higher exogenous organic C uptake activities [43]. Ancient aquatic species-related [44] microbial biofilms [45] and UV-resistant microorganisms [46,47] are discovered from the Atacama Desert. These organic sources should persist for a long time [48]. With little external input, leaching and subsurface decomposition [42], organic C in Atacama soils should mostly derive *in situ*. Thus, organic C contents can directly reflect the active biomass of native microbial communities.

The majority of previous investigations into microbial N cycling have focused on marine or terrestrial environments, where liquid water is abundant or non-limiting and nitrate is aqueous or easily solubilized [49,50]. Here we investigate the effects of nitrate on microbial growth in a hyperarid-arid Mars analog environment, to investigate how microorganisms survive in a water-limited, oligotrophic environment with high levels of nitrate [16]. We combine a number of geochemical and microbiological methods to study how nitrate accumulation as a result of rain limitation and long-term atmospheric deposition impacts the microbial abundance and growth rates in these soils.

2. Materials and Methods

97 *2.1. Study sites*

98 Seven sites were sampled in the Atacama Desert, on a latitudinal gradient from 22°S to 29°S
99 (Figure 1), between the 30th Nov and 6th Dec of 2017, half a year after an unprecedented rainfall event
100 (centered on the region of Yungay, during 5th to 8th Jun of 2017) [17]. From the hyperarid north to the
101 arid south, the sites are María Elena South (MES), Point of No Return Dos (PONR-2), Yungay,
102 Transition Zone 0 (TZ-0), Transition Zone 4 (TZ-4), Transition Zone 5 (TZ-5), and Transition Zone 6
103 (TZ-6). In each site, 3 pits were dug to 20 cm depth for sampling. Samples for geochemical analyses
104 were sampled from homogenized 10 to 20 cm depth with non-sterilized spades and collected in
105 clean plastic bags. Samples for cell spreading experiments were sampled at one sampling pit at each
106 site with ethanol-sprayed spades and collected in sterile Whirl-Pak® bags (Nasco, Fort Atkinson,
107 USA).

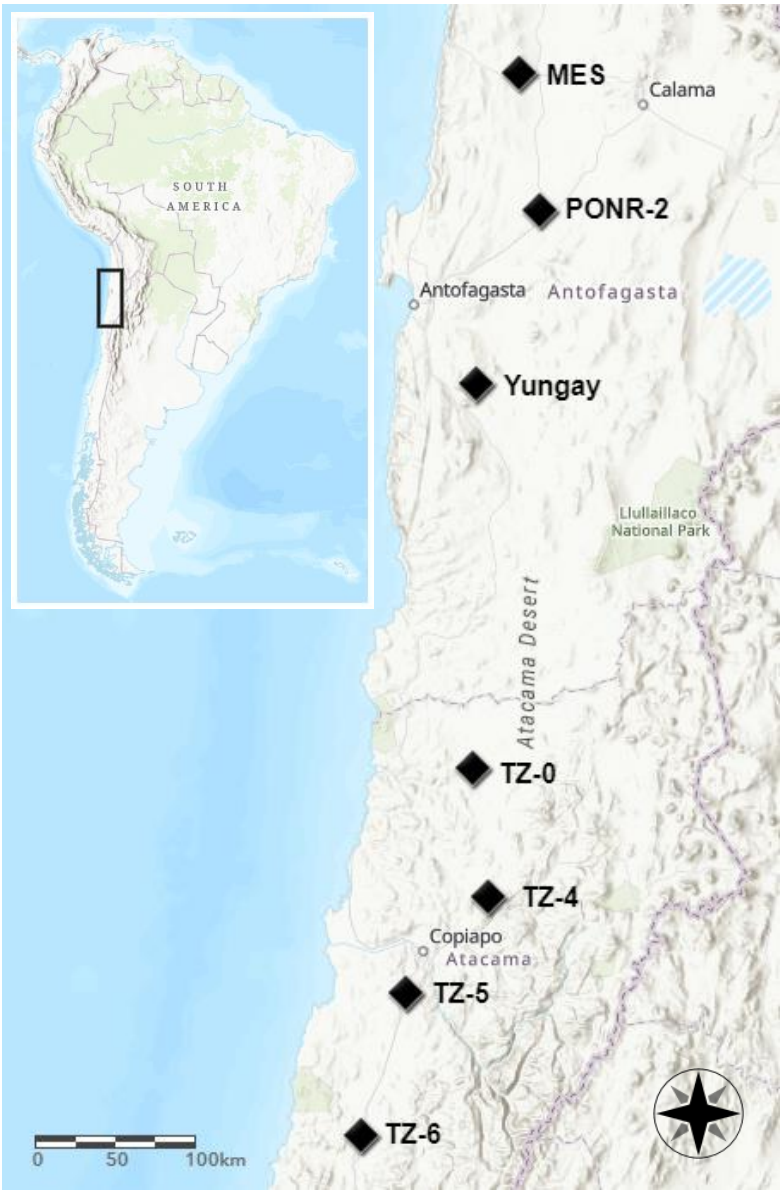

108 **Figure 1.** Seven study sites (MES, PONR-2, Yungay, TZ-0, TZ-4, TZ-5, and TZ-6) from the Atacama
109 Desert, northern Chile.

110 Rainfall was the most important environmental variable we chose for site characterization.
111 Annual precipitation information (Table 1) for each sampling site was determined from the nearest
112 rain gauge(s) between the years of 1940 and 2017 (the sampling date) from Explorador Climático,
113 Center for Climate and Resilience Research (http://explorador.cr2.cl/). Daily precipitation during the
114 unprecedented rainfall event (5-8 Jun 2017) was also recorded, although we acknowledge that the

gauging station data are quite sparse in the hyperarid core of the desert, and there may be local heterogeneity in rainfall distribution.

Table 1. Site characterization (showing terrestrial coordinates, altitude, estimated annual precipitation, grain size (mean ± SD), SiO_2/Al_2O_3 ratios, pH, and electrical conductivity).

Site	Latitude	Longitude	Altitude (m)	Precipitation (mm/yr)	Precipitation (mm/day) (5-8 Jun 2017)	pH	Conductivity (mS/cm)	Grain size (μm)	SiO_2/Al_2O_3	NO_3 (ppm)	TOC (ppm)	TN (ppm)
MES	S 22° 15' 50.7"	W 69° 43' 27.3"	1493	0.7	0.4	9.5	6.6	520±325	4.47	110	59	29
PONR-2	S 23° 04' 21.3"	W 69° 35' 21.1"	1493	1.1	2.9	9.2	19	564±438	3.96	220	94	61
Yungay	S 24° 05' 18.4"	W 69° 59' 40.1"	1007	2	5.3	9.1	18	572±563	3.96	20	76	42
TZ-0	S 26° 19' 19.9"	W 70° 00' 46.2"	1106	10	1.7	10.5	0.94	561±379	3.94	1.9	120	42
TZ-4	S 27° 03' 23.4"	W 69° 55' 22.0"	1658	15	2.9	9.2	19	324±155	3.66	5000	210	88
TZ-5	S 27° 36' 18.4"	W 70° 26' 44.9"	588	20	2.1	10.1	8.4	437±335	4.47	10	790	89
TZ-6	S 28° 24' 36.0"	W 70° 43' 37.3"	658	30	0.6	10.1	8.0	503±342	4.30	78	1400	170

2.2. Soil characterization

The pH of soils was measured in triplicate by FiveGo pH meter F2 (Mettler Toledo, Columbus, Ohio, USA) and the electrical conductivity was measured in triplicate by HI-98129 Pocket EC/TDS meter (Hanna Instruments Ltd, Leighton Buzzard, England) (Table 1).

X-ray fluorescence (XRF) was conducted for major element determination. For XRF analysis, soil samples were crushed using a Planetary Micro Mill PULVERISETTE (FRITSCH, Germany) and sieved through a 355 μm sieve. The sieved samples were first combusted to eliminate all organics, sulfur, water and other volatiles. Ashed samples were fused with Lithiumtetraborate 50% / Lithiummetaborate 50% (T50/M50) (FLUXANA, Scientific & Medical Products Ltd, Stockport, England). Major elements were determined on fused pellets using a SPECTRO XEPOS XRF Spectrometer (SPECTRO Analytical Instruments, Kleve, Germany). Counting errors were determined in comparison with the errors in the calibration. The deviations on the BR, GSP-2, and NIST SRM 2711 standards [51] were used for accuracy and precision assessments.

High-resolution pictures of soils that were washed to clear the dust coverage were taken under a VHX-2000 Digital Microscope (KEYENCE UK & Ireland) (Figure S1a, c, e, g, i, k & m). Four view fields were randomly chosen from each soil sample. Diameters of fifty particles were measured from each view field. In total, 200 particle diameters from each site were measured as a reference of grain size (Figure S1b, d, f, h, j, l & n).

2.3. Nitrate measurements

Soil samples for nitrate concentration measurements were sieved with a 1.4 mm stainless steel sieve. To extract the nitrate, sieved samples were suspended and mixed well in 18.2 MΩ/cm resistance ultrapure water (Merck Millipore, Burlington, Massachusetts, USA) using a 10:1 dilution factor, and shaken for 45 minutes at 200 rpm at 40°C. After centrifugation at 4,000 rpm for 10 min,

the supernatant of the soil suspension was filtered through a 0.20-micron filter. All implements that touched samples were triple rinsed in ultrapure water prior to contact. Nitrate concentrations were measured in triplicate on this filtered solution by Ion Chromatography via a Metrohm 930/889 IC/Autosampler (Metrohm AG, Switzerland), with a 150 mm Metrosep A Supp 5 separation column (4 mm bore) using 3.1 mM Na_2CO_3 / 1 mM $NaHCO_3$ eluent at a flow rate of 0.7 mL/min. Peak areas were calibrated for nitrate concentrations with nine standards prepared in laboratory and measured in triplicate by the same Ion Chromatography method.

2.4. Total organic carbon (TOC) and total nitrogen (TN)

For TOC and TN analyses, finely-ground soil samples were decarbonated by adding 2 M HCl and sonicating for 30 min. Extra HCl was removed by washing three times with ultrapure water. All soluble salts, including nitrate, were similarly washed away after decarbonation. Hence our TN measurements do not include nitrate but only organic- and clay-bound nitrogen. TOC and TN were measured in an elemental analyzer (EA) Isolink coupled to a MAT253 isotope ratio mass spectrometer (IRMS) via a Conflo IV (Thermo Fischer Scientific, Bremen, Germany) in triplicate. Peak areas were calibrated for C and N abundances with multiple aliquots of the international reference material USGS-41. Isotopes will not be reported in this study.

2.5. Nitrate amendments and colony forming units (CFUs)

About 10 g of our sterilely-collected soil from each sampling site was amended with 4.5 mL of sterilized 10% sodium nitrate and 4.5 mL of sterilized ultrapure water (as a control) and left for 4 days at 21°C. Soils were then refrigerated at 4°C. Duplicate amended soils and original soils without amendments were suspended in sterilized ultrapure water by an applicable dilution factor and spread on ultrapure agarose (15 g/L Agarose), Luria-Bertani agar (15 g/L Agar, 10 g/L Tryptone, 5 g/L Yeast Extract, 5 g/L NaCl), and plate count agar (9 g/L Agar, 1 g/L Dextrose, 5 g/L Tryptone, 2.5 g/L Yeast Extract) plates, sealed, and left at 21°C. Colonies were counted after 20 days of growth [27]. CFUs were calculated by multiplying the number of colonies formed on agar plates by the corresponding dilution factor, and a factor 1.45 to account for the addition of 4.5 mL of solution to 10 g of soil. The relative microbial growth rate is defined as the difference of CFUs between samples inoculated with nitrate amendments and those treated with water only (controls) on a logarithmic scale.

2.6. Principal component and multiple regression analyses

Data from sampling sites were analyzed using the OriginPro 2018 software [52] by principal component analysis (PCA) using XRF results (Table S1), TOC, TN, and mean annual precipitation as primary environmental variables. Since the annual precipitation only has one column input to the PCA analysis but it is the most fundamental variable in this study, we used the two principal components that assign the highest weight to precipitation for site clustering.

Multiple regressive analyses were run using IBM SPSS Statistics 25 software [53] to examine statistical bases for the following: (1) how mean annual precipitation, grain size, and quartz to clay ratios affect nitrate distribution across a humidity gradient; and (2) how rain and nitrate affect TOC or culturable cell counts.

2.7. Path analyses

In addition to measurable variables, countless latent variables exist. We therefore applied path analysis to our data, which can provide a more unbiased summary analysis covering variance-covariance, correlation, and regression, usually used in social sciences [54], biological sciences [55], and medical sciences [56]. Path analysis can elucidate complex dependency or codependency in a structural diagram, and provides a useful tool to help avoid false collinearity and model oversimplification [57].

In this study, path analyses were conducted in the IBM SPSS Amos 25 Graphics software [58]. In the resulting plots, measured (observed) variables are represented by rectangles, while latent (unobserved) variables are represented by round shapes. Latent variables are potential unknown factors that could affect their targeted dependent variables and are referred to as "other" followed by an ordered number. Single-headed arrows point from independent variables to the dependent variable of regression analyses. The numbers on arrows indicate their regression weight; the regression weights of latent variables were assigned to 1 at the beginning for standardization.

For the path analysis including CFUs, rain, nitrate and culturable cell counts, measured variables were transformed with a logarithmic function. Path analysis was conducted for estimating variances and regression weights of annual precipitation, native nitrate, and TOC on the relative growth rate of the soil microorganisms on cell culture plates amended with excessive nitrate.

Annual precipitation may affect all the other variables, including native nitrate concentrations, culturable microbes, and the response pattern of microbes to excessive nitrate amendments. Native nitrate levels may also affect the culturable microbes and microbial response pattern to nitrate amendments. Original culturable biomass may affect the response of the relative growth rates to nitrate amendments. Single-headed arrows were drawn to illustrate these potential paths of interdependence; their regression weights are marked with * symbol when the relationship is statistically significant at α= 0.05 level, ** when statistically significant at α= 0.01 level, and *** when statistically significant at α= 0.001 level.

Each measured variable is associated with one latent independent variable for detecting any unknown factors that may directly affect the analyses. For example, "other1" refers to any errors that are associated with rainfall data recorded by the closest climate station, "other2" to "other6" refer to the unknown environmental factors (e.g., cation availability and many more) that may affect nitrate concentration, biomass cultured on agar plates, and microbial relative growth rate to nitrate amendments, respectively. The number listed beside each of the round shapes is the greatest variance of the latent variable that allows them to have a 0.083 significance level, which is deemed not too significant to overwhelm the effects of measured variables.

An additional path analysis was conducted in the same manner to summarize the dependency relationships among annual precipitation, sedimentation rates, native nitrate concentrations, TOC, and TN.

3. Results

3.1. Physical and chemical properties of the soils

Bulk physical and chemical properties of the Atacama soils at 10-20 cm depth are listed in Table 1. The measured pH in our study sites was between 9 and 10.5, and electrical conductivity varied from 0.9 to 20 mS/cm. Mean grain size varied from 324 μm in TZ-4 to 572 μm in Yungay. The standard deviation in grain size is the lowest in TZ-4 and highest in Yungay.

On average, the sampled soils were composed of about 54.0% silicon (Si), 13.2% aluminium (Al), 7.9% calcium (Ca), 5.4% iron (Fe), 3.1% sodium (Na), 2.3% magnesium (Mg), 2.3% potassium (K), 0.65% titanium (Ti), 0.22% phosphorus (P), and 0.11% manganese (Mn) (Table S1). The SiO_2/Al_2O_3 ratios varied from 3.5 (TZ-4) to 4.5 (MES and TZ-5) (Table 1).

Nitrate concentrations were highly variable, ranging from 2 ppm (at TZ-0) to 5,000 ppm (at TZ-4) (Table 1). Nitrate distribution varied amongst the individual sites, but did not show any significant correlation with both mean annual precipitation and the recent heavy rainfall (Figure 2). Site TZ-4 in particular has an extremely high nitrate concentration. TOC and TN concentrations ranged from 50 to 1,500 ppm and from 20 to 200 ppm, respectively (Table 1).

Preprints (www.preprints.org) | NOT PEER-REVIEWED | Posted: 25 July 2019 doi:10.20944/preprints201907.0292.v1

Peer-reviewed version available at Life 2019, 9, 79; doi:10.3390/life9040079

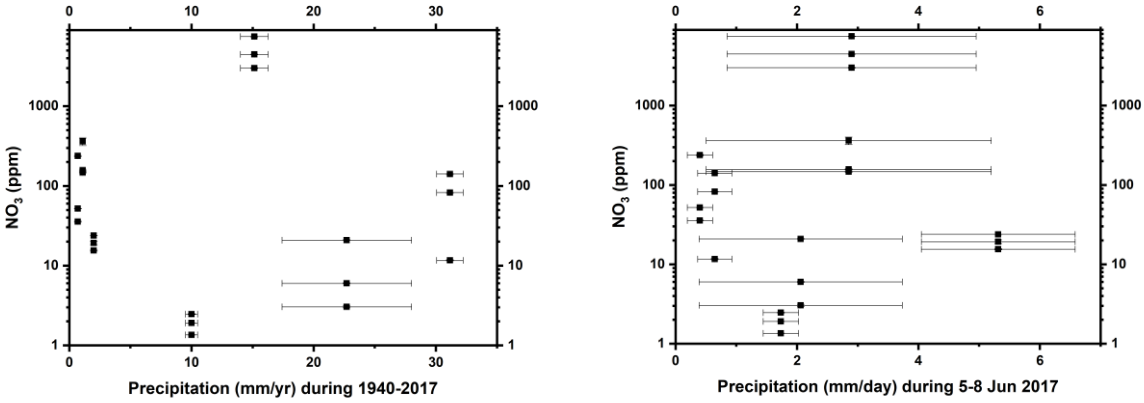

(**a**) (**b**)

Figure 2. The distribution pattern of nitrate as a function of (**a**) mean annual precipitation (1940-2017) and (**b**) daily precipitation (5-8 Jun 2017) in the Atacama Desert.

3.2. Site categorization

Principal components 1 and 3 assign the highest weight to rain (0.89 and 0.37, respectively), so we used these two components to cluster the 7 sampling sites. Following this method, 3 clusters emerge: (1) sites with high Si, Al, Ca, Na but low annual precipitation (sites MES, PONR-2, and Yungay); (2) sites with slightly more mafic minerals characterized by slightly elevated levels of Fe, Mg, Mn, Ti, loss on ignition (LOI) and intermediate annual precipitation (sites TZ-0 and TZ-4); and (3) sites with high K, P, TOC, TN, and annual precipitation (sites TZ-5 and TZ-6) (Figure 3). We therefore refer to MES, PONR-2, and Yungay as "hyperarid" sites; TZ-0 and TZ-4 as "intermediate" sites; and TZ-5 and TZ-6 as "arid" sites, which broadly captures the changes evident within other aridity indexes such as the evaporation/precipitation ratios.

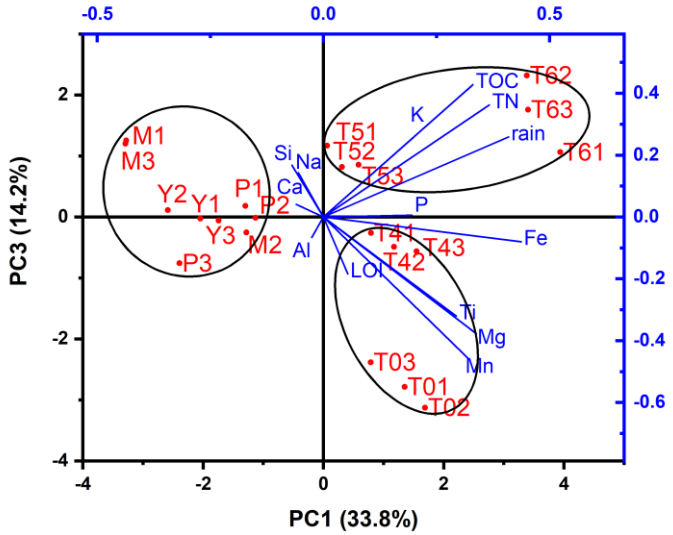

Figure 3. Principal component analysis of sites based on major elements in the regolith, total organic carbon (TOC), total nitrogen (TN), and annual precipitation. Principal components 1 and 3 assign the highest weights to annual precipitation. We refer to the 3 sampling pits from MES as M1, M2, M3; PONR-2 as P1, P2, P3; Yungay as Y1, Y2, Y3; TZ-0 as T01, T02, T03; TZ-4 as T41, T42, T43; TZ-5 as T51, T52, T53; TZ-6 as T61, T62, T63.

3.3. Cell counts on agar plates

Results of CFU counts are shown in Table 2. On ultrapure agarose plates, CFU counts ranged from 0 to 1.62×10^3 without any amendments, from 0 to 3.57×10^3 on water control, and from 2 to

3.15×10^3 with nitrate amendments. On Luria-Bertani agar plates, CFUs ranged from 17 to 2.39×10^5 without amendments, from 7 to 1.23×10^6 on water control, and from 0 to 3.27×10^5 with nitrate amendments. Growth occurred on all plate count agar plates, with CFUs ranging from 167 to 2.90×10^6 without amendments, from 1.36×10^3 to 1.33×10^7 on water control, and from 15 to 2.47×10^6 with nitrate amendments.

Table 2. Colony forming units (CFUs) on ultrapure agarose, Luria-Bertani agar, and plate count agar plates without amendments, amended with water only, and amended with 10% sodium nitrate.

Type of culture plate	Amendment	MES	PONR-2	Yungay	TZ-0	TZ-4	TZ-5	TZ-6
Ultrapure agarose	No	0	17	13	93	1.62×10^3	80	1.42×10^3
	Water	0	15	106	111	3.57×10^3	87	667
	Nitrate	2	2	7	1.33×10^3	3.15×10^3	1.62×10^3	2.93×10^3
Luria-Bertani agar	No	17	28	33	91	2.39×10^5	2.95×10^3	5.41×10^4
	Water	7	7.98×10^3	3.71×10^3	491	1.23×10^6	1.17×10^3	1.54×10^5
	Nitrate	0	9.43×10^3	197	290	4.88×10^3	1.00×10^4	3.27×10^5
Plate count agar	No	167	190	5.17×10^3	353	2.90×10^6	6.00×10^3	2.72×10^5
	Water	1.36×10^3	8.56×10^4	6.96×10^4	638	1.33×10^7	1.25×10^5	4.12×10^6
	Nitrate	15	44	29	343	2.47×10^6	6.96×10^4	5.22×10^5

4. Discussion

4.1. Nitrate distribution and effects on microbial N assimilation

Soil samples of this study are collected at a depth of about 10 to 20 cm. This depth is not as sensitive as the surface to geochemical input and output processes. Biosignatures are relatively preservative at the shallow subsurface, as it is not easily transportable by wind and not directly exposed to the extreme UV stress [28,30,33,39,59,60].

We characterized the 7 study sites into 3 clusters, based on the geochemical trends described above: the hyperarid sites, including MES, PONR-2, and Yungay; the mafic intermediate sites, including TZ-0 and TZ-4; and the arid sites, including TZ-5 and TZ-6 (Figure 3). The hyperarid core of the Atacama Desert can be described as an analog to the late Hesperian/Amazonian Periods [61] on Mars [4], with low humidity and large nitrate reservoirs. The arid and transitional sites, on the other hand, are more analogous to regions of Mars where humidity or organic C levels might be slightly elevated, perhaps analogous to a Noachian Mars [61]. Therefore, comparisons between the hyperarid sites and arid/transitional sites provides insight into the strategies that potentially extant microorganisms on Mars might use to respond to changes in humidity and nitrogen input.

Nitrate concentrations in our samples do not directly scale with precipitation estimates, as might be expected (Figure 2). The massive rainfall events ~6 months prior to our sampling would presumably have leached away the majority of nitrate in the shallow subsurface of the affected sites, contributing to the high variability in the distribution of nitrate across our sampling sites (Figure 2b). It is certainly possible that the massive rainfalls did not efficiently affect site TZ-4, although dead brush and presence of small desiccated roots hint that a desert bloom (*desierto florido*) may have occurred at the site prior to our sampling, which may have affected near-surface nitrate levels.

However, additional physicochemical factors could also account for this seemingly random nitrate distribution. The inferred more humid intermediate site TZ-4 has ten to one hundred times higher nitrate concentrations than the other sampled Atacama sites, but it also has smaller average grain sizes and lower SiO_2/Al_2O_3 ratios (Table 1). Sedimentation rates, which in this case mostly reflect the influx of wind-blown dust as indicated by the moderate roundedness and frosting of the grains (Figure S1), can be inferred from grain size distribution and SiO_2/Al_2O_3 (approximating quartz to clay) ratios in these soils: quartz is heavier (~2.65 g/cm^3 compared to clay density ~1.33 g/cm^3) and

thus less likely to be deposited in a low-energy environment where only small particles are transportable. This comparison therefore suggests that site TZ-4 has a significantly lower sedimentation rate than other sites sampled. Lower sedimentation rates would mean corresponding less dilution of atmospheric nitrate by terrigenous input, and correlatively higher nitrate levels. Multiple regression analyses suggest that grain size (Figure S1 & Table 1) (standardized coefficient= -0.77***, p= 0.000) and SiO_2/Al_2O_3 (standardized coefficient= -0.42**, p= 0.001) are more directly correlated with nitrate concentrations at all sampling sites compared to annual precipitation (standardized coefficient= -0.16, p= 0.207). Therefore, we speculate that in addition to annual precipitation, other physical factors such as sedimentation rates can also significantly influence the nitrate distribution in Atacama, and by proxy Martian, soils.

The distribution of TOC, as an approximate quantification of biomass, increases along with annual precipitation (Figure 4a) as long-term biomass preservation, indicating that water is a limiting factor for microbial growth, as expected. Total nitrogen (TN) is positively correlated with TOC with a small intercept of 40 ppm on the TN-axis (Figure 4b), indicating that the majority of nitrogen in these soils is organic-bound rather than substituting for potassium in detrital clay minerals. The small fraction of 40 ppm clay-bound N may be derived from *in-situ* degradation of biomass, analogous to processes described from marine sediments [62,63]. This interpretation is validated by a lack of correlation between TN and potassium (Figure S2). We can therefore refer to the non-soluble N in our soils as total organic nitrogen (TON).

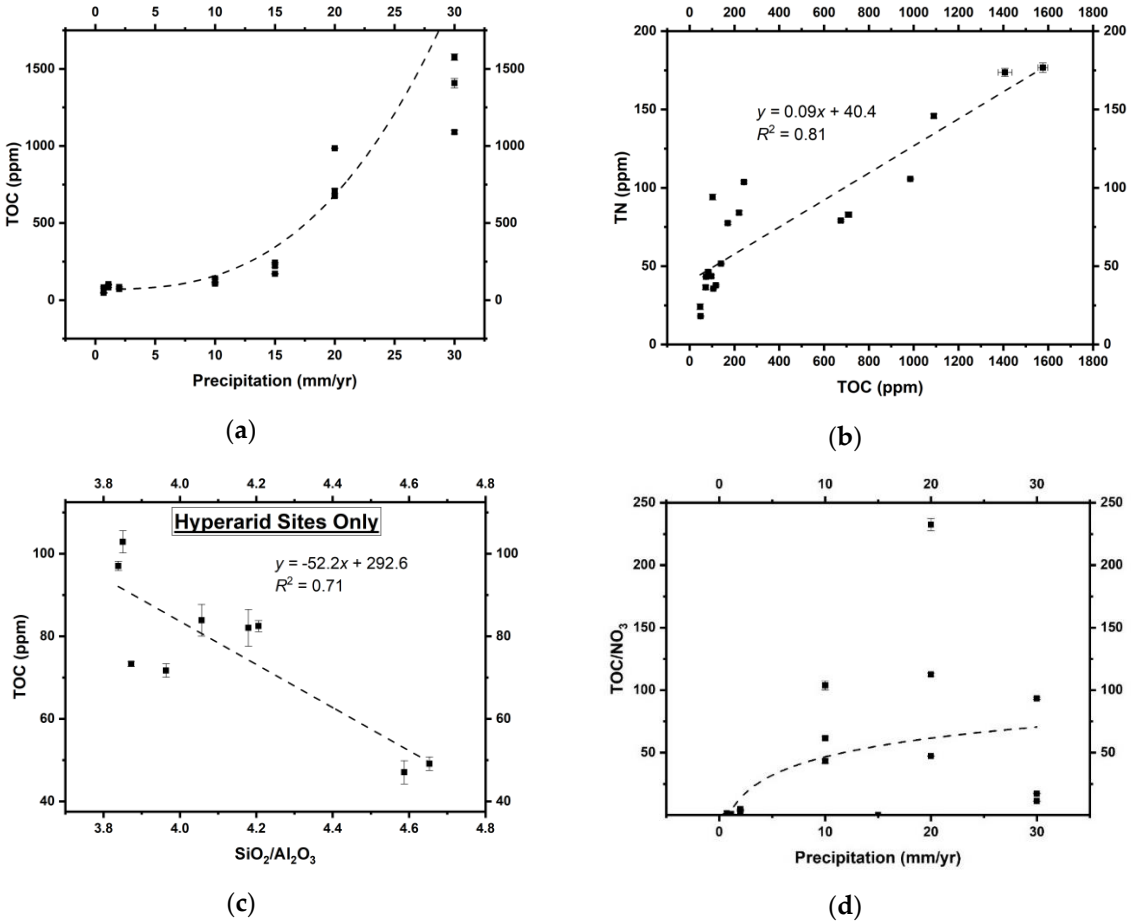

Figure 4. (**a**) TOC versus inferred annual precipitation; (**b**) TOC versus TN; (**c**) TOC versus SiO_2/Al_2O_3 (approximating quartz/clay) ratio in the core Atacama Desert; (**d**) Annual precipitation versus TOC/nitrate ratios.

Furthermore, an anti-correlation between quartz to clay ratios and TOC in the core of the Atacama Desert (Figure 4c) suggests that lower quartz/clay ratios lead to less dilution of the soil TOC contents produced by microbial communities *in situ*. Given the potential dilution effect of

Peer-reviewed version available at Life 2019, 9, 79; doi:10.3390/life9040079

sedimentation rates on nitrate concentrations discussed above, these results suggest that a greater proportion of clays (i.e., lower quartz/clay ratios) in hyperarid sediments could also enhance biomass preservation, consistent with previous studies suggesting that clay minerals could constitute a microniche suitable for the preservation of biochemical materials [64-66].

In order to access nitrate, microorganisms generally need water to dissolve and solubilize nitrate salts and other bioessential molecules in the soil. In more humid environments, nitrate availability to organisms generally scales with nitrate richness, leading to higher microbial abundance at higher nitrate levels. At the hyperarid core of the Atacama Desert where rainfall is almost absent, TOC (approximating biomass) positively correlates with both annual precipitation (standardized coefficient= 0.65*, p= 0.019) and nitrate concentrations (standardized coefficient= 0.98**, p= 0.003). These trends suggest that nitrate concentrations remain as important as rainfall for microbial abundance in the most Mars-analogous environments. On the other hand, when annual precipitation exceeds 10 mm, the positive effect of nitrate on microbial abundance declines (Figure 4d). In spite of the strong rainfall control on microbial metabolic activities, nitrate to TOC ratios (as a representative of the probability for microbes to encounter nitrate) are positively associated with TON in all the hyperarid, intermediate, and arid sites of the Atacama Desert (Figure 5). This suggests that microbial communities with a higher probability to contact nitrate can assimilate nitrate more quickly for metabolism and biomass production, regardless of precipitation.

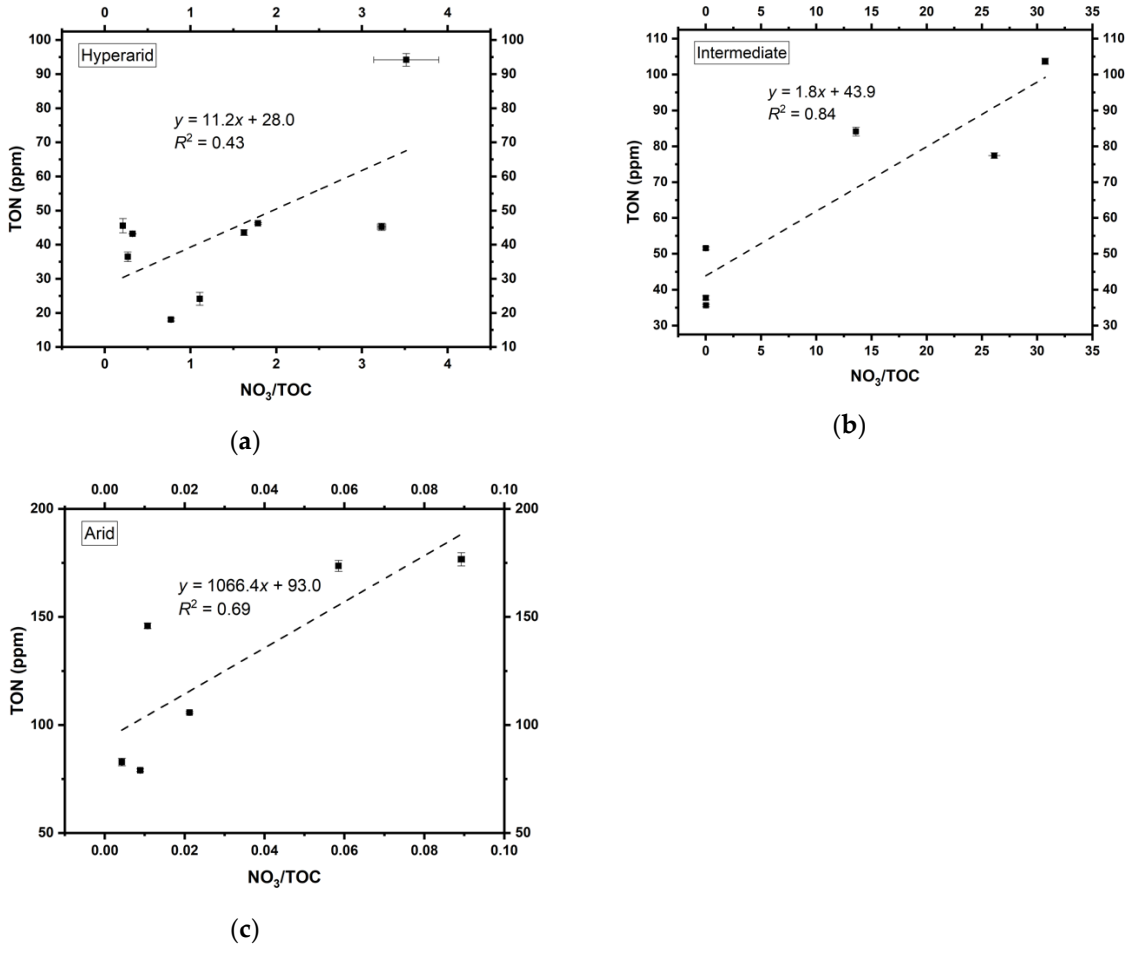

Figure 5. The effect of nitrate to organic C ratio on N assimilation at the (**a**) hyperarid, (**b**) intermediate, and (**c**) arid sites.

In summary, both the mean annual precipitation (as a long-term regulator of both nitrate and biomass) and sedimentation rates negatively control nitrate concentration. Sedimentation rates additionally can dilute TOC. The significant positive correlation between the indigenous nitrate

concentrations and TON contents indicates that nitrate is likely used by microorganisms for assimilation (Figure 6).

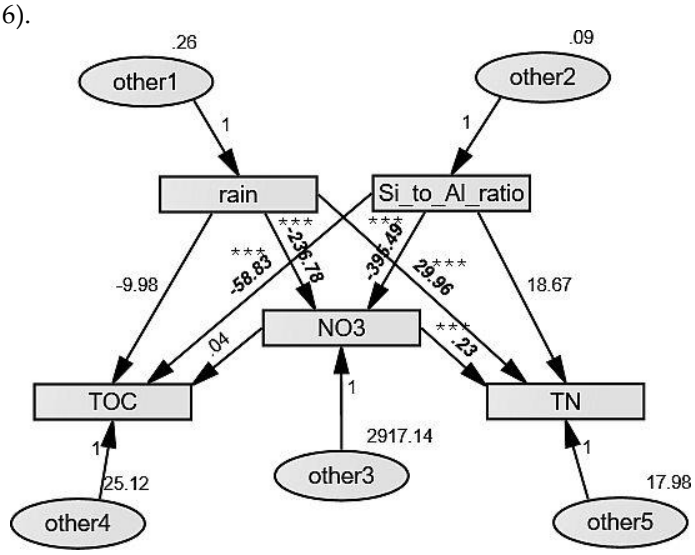

Figure 6. Path diagram of the variances and regression weights of rain, sedimentation rates (silicon to aluminium ratios as a quantitation), nitrate, and TOC, and TN (or TON) in the hyperarid sites.

4.2. Growth of cell cultures with nitrate amendments

We tested the interpretations above with laboratory experiments designed to investigate the importance of these variables on microbial growth as estimated from CFUs inoculated from Atacama soils. Discussions of the effects of water amendments on microbial growth are beyond the scope of this paper, but we will examine them in future work. Overall, mean annual precipitation and local nitrate concentrations are both positively correlated with CFUs on all ultrapure agarose (standardized coefficient of rain= 0.59*, p= 0.042, standardized coefficient of NO_3= 0.62*, p= 0.036), Luria-Bertani agar (standardized coefficient of rain= 0.19*, p= 0.034, standardized coefficient of NO_3= 0.95***, p= 0.000), and plate count agar plates (standardized coefficient of rain= 0.08*, p= 0.034, standardized coefficient of NO_3= 0.98***, p= 0.000).

However, the distribution of cultivable heterotrophic CFUs illustrates that no microbial communities show a significant preference for excessive nitrate amendments, if more than one order of magnitude change is defined to be significant. In comparison to the arid sites and TZ-0, nitrate amendments have a more negative effect on the relative microbial growth rate at the hyperarid sites and TZ-4 (Table S2). These results seem to confirm that in wetter sites with relatively low nitrate levels, native microbial communities generally prefer higher nitrate inputs and have a higher nitrate tolerance; while in drier sites, extreme excess nitrate may cause damage to microorganisms due to its oxidative activity and osmotic stress [67-69]. Thus, the significant correlation between annual precipitation and total CFUs as well as the microbial response pattern to nitrate amendments (Figure 7) is presumably a result of nitrate bioavailability enhanced by solubilization during precipitation.

Peer-reviewed version available at Life 2019, 9, 79; doi:10.3390/life9040079

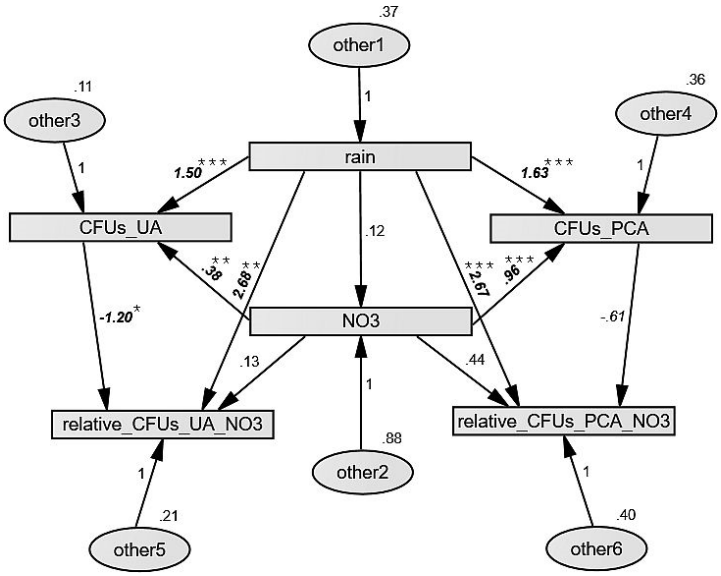

Figure 7. Path diagram of the variances and regression weights of rain, nitrate, and original biomass on agar plates and the relative microbial growth rate on agar plates with excessive nitrate amendments. All variables are scaled by using logarithmic transformation. (CFUs_UA, colony forming units counted on ultrapure agarose plates; CFUs_PCA, colony forming units counted on plate count agar plates; relative_CFUs_UA_NO3, the relative colony forming units on nitrate-amended ultrapure agarose plates; relative_CFUs_PCA_NO3, relative colony forming units on nitrate-amended plate count agar plates). *p<0.05, **p<0.01, ***p<0.001

4.3. Relevance for past and present life on Mars

Approximately 4.1 to 3.0 billion years ago (Noachian and early Hesperian Periods) [70,71], the existence of ancient Martian deltas, paleolake basins, and carved outflow channels suggests that Mars was a more humid planet potentially even supporting oceans [72,73], rivers, lakes [74,75], and possibly rainfall [76]. Given the importance of water for biochemical functions, life presumably could have evolved and thrived during that period. If so, during the transition to an extremely hyperarid planet, Martian life could have been faced with harsh conditions similar to those experienced by microbial communities in the Atacama Desert for more than hundreds of millions of years. In such a dry, oligotrophic environment, only extremophilic life that is tolerant of desiccation, irradiation, and high salinity could potentially survive and even reproduce [77]. To achieve this, extremophiles would have needed to develop strategies to take advantage of ambient N sources, such as atmospherically-derived nitrate salts.

Our results from Atacama soils suggest that potentially extant Martian life could survive under the high levels of nitrate availability [3,14,15]. On Mars, the concentrations of nitrate and TOC should be even more tightly regulated by local sedimentation rates, since modern Mars does not have detectable rainfall. Without rainwater to solubilize nitrate, any organisms present near the surface on Mars should not be experiencing the high nitrate stress suggested by our culturing experiments, because the nitrate availability remains nearly stable. We suggest that sustained high nitrate availability in Martian sediments could potentially provide a sufficient nutrient source to support life over geological timescales spanning the decline of the wet early Mars to modern hyperarid Mars.

5. Conclusions

Here we present a pioneering study to investigate the effects of atmospherically-derived nitrate on biomass and microbial growth in an infertile Mars analog environment (the Atacama Desert) with extremely low humidity, high UV irradiation, and large nitrate reservoirs. It is intriguing to discover that higher nitrate to biomass ratios seem more beneficial to microbial growth and N assimilation within all sites sampled (Figure 6). Both precipitation and dilution of nitrate with

terrigenous sediments seem to be important controls on nitrate concentrations in arid regions. On Mars, nitrate should be primarily regulated by sedimentation and act as the only N source to microorganisms (probably irradiation-resistant and halophilic prokaryotes [39]). Higher nitrate levels are a sign of habitability, which might be a useful guide for future life detection on Mars.

Supplementary Materials: The following are available online at www.mdpi.com/xxx/s1.

(**a**)

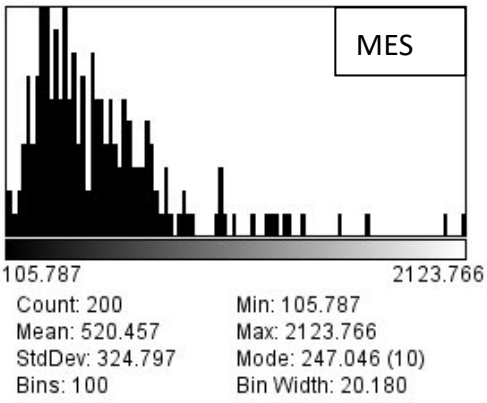

(**b**)

(**c**)

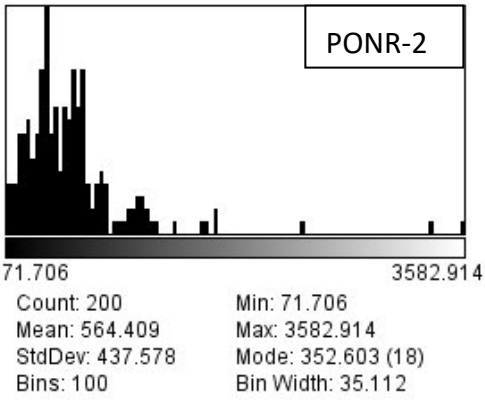

(**d**)

(**e**)

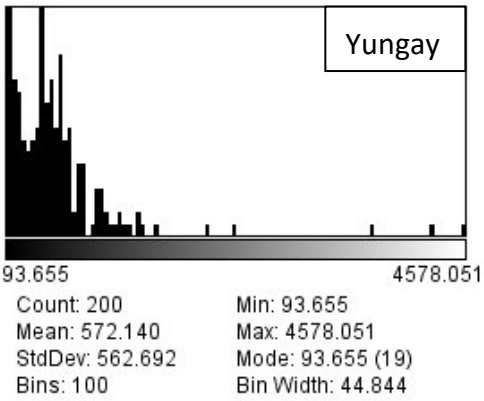

(**f**)

Preprints (www.preprints.org) | NOT PEER-REVIEWED | Posted: 25 July 2019 doi:10.20944/preprints201907.0292.v1

Peer-reviewed version available at Life 2019, 9, 79; doi:10.3390/life9040079

(g)

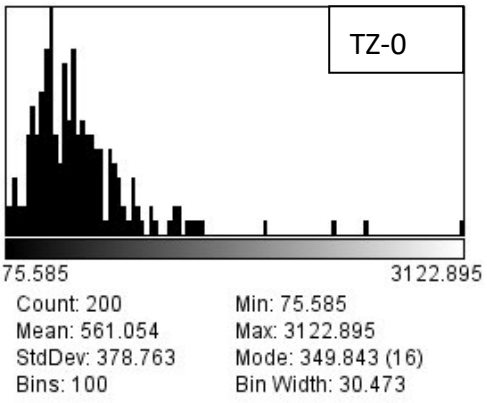

(h)

(i)

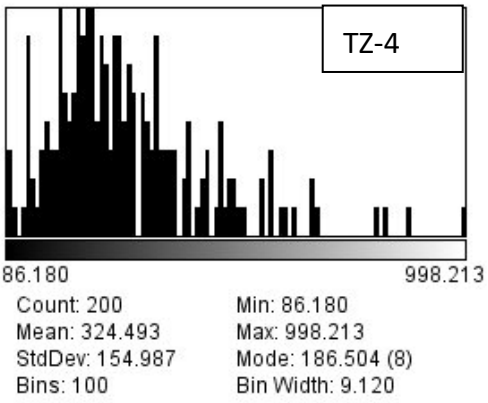

(j)

(k)

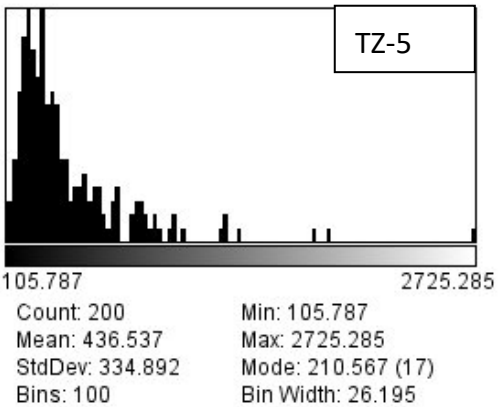

(l)

(m)

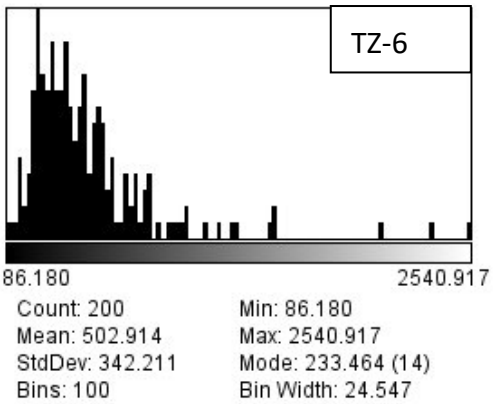

(n)

Peer-reviewed version available at *Life* **2019**, *9*, 79; doi:10.3390/life9040079

Figure S1. Microscopic visualization and grain size distribution of (**a** & **b**) MES, (**c** & **d**) PONR-2, (**e** & **f**) Yungay, (**g** & **h**) TZ-0, (**i** & **j**) TZ-4, (**k** & **l**) TZ-5, and (**m** & **n**) TZ-6.

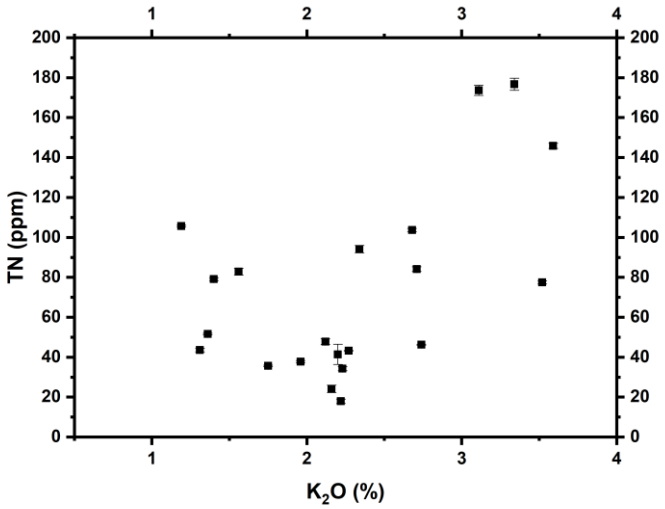

Figure S2. No correlation between TN and potassium, indicating TN is not clay-bound. Since ammonium is usually trapped by clay along with potassium, clay-independent TN suggests this TN is mostly organic.

Table S1. Detailed major element components of sampling pits. We refer to the 3 sampling pits from MES as M1, M2, M3; PONR-2 as P1, P2, P3; Yungayt as Y1, Y2, Y3; TZ-0 as T01, T02, T03; TZ-4 as T41, T42, T43; TZ-5 as T51, T52, T53; TZ-6 as T61, T62, T63. (LOI, loss on ignition)

Pit name	SiO_2 %	TiO_2 %	Al_2O_3 %	Fe_2O_3 %	MnO %	MgO %	CaO %	Na_2O %	K_2O %	P_2O_5 %	LOI %
M1	69.05	0.39	14.84	2.92	0.05	1.27	3.31	4.19	2.22	0.13	1.43
M2	62.48	0.68	14.95	5.29	0.09	2.22	4.56	3.55	2.12	0.16	3.49
M3	67.94	0.36	14.81	2.81	0.05	1.34	3.79	3.94	2.16	0.12	2.38
P1	64.05	0.74	15.23	4.44	0.08	1.27	3.8	2.93	2.74	0.26	3.86
P2	51.48	0.6	13.37	4.26	0.07	1.65	8.57	2.41	2.34	0.2	13.11
P3	33.78	0.52	8.8	3.29	0.06	1.03	16.91	1.69	1.31	0.11	17.36
Y1	47.01	0.67	12.14	3.68	0.06	1.21	11.83	3.31	2.27	0.08	10.41
Y2	47.88	0.48	12.08	2.88	0.06	1.09	11.24	2.9	2.23	0.09	14.65
Y3	52.45	0.78	12.93	4.23	0.07	0.99	9.57	3.48	2.2	0.11	7.96
T01	53.32	0.98	13.62	6.63	0.24	3.43	6.72	3.29	1.96	0.23	9.34
T02	49.66	0.79	12.02	8.17	0.23	4.81	7.99	3.05	1.36	0.18	11.52
T03	53.48	0.78	14.2	6.75	0.23	3.71	6.29	3.79	1.75	0.17	8.59
T41	57.88	0.65	15.4	5.39	0.13	2.78	3.54	2.54	2.71	0.38	8.38
T42	53.33	0.58	15.02	5.18	0.14	3.21	5.28	2.09	2.68	0.44	11.8
T43	54.01	0.71	14.76	6.6	0.15	3.3	4.05	3.01	3.52	0.35	9.2
T51	55.99	0.55	12.47	5.49	0.08	1.92	10.92	3.46	1.56	0.34	6.93
T52	55.79	0.63	12.57	5.84	0.09	2.06	9.67	3.96	1.4	0.36	7.37
T53	44.37	0.49	9.92	5.21	0.07	2.7	17.26	3.03	1.19	0.37	14.75
T61	57.35	0.86	13.56	9.47	0.17	2.86	3.34	3.12	3.59	0.22	5.17
T62	50.1	0.71	11.5	8.02	0.13	2.52	9.38	3.66	3.34	0.14	10.18
T63	52.25	0.76	12.09	7.7	0.13	2.62	8.48	2.7	3.11	0.2	9.65

Table S2. Results of cell culture on ultrapure agarose, Luria-Bertani agar, and plate count agar plates with or without excessive nitrate amendments, illustrating relative microbial growth rate with nitrate amendments (all variables are scaled by logarithmic transformation). Negative effect of nitrate on microbial growth more than one order of magnitude is marked as bold. In general, microbial community from arid sites has a higher tolerance or preference for nitrate addition.

Precipitation (mm/yr)	NO_3 (ppm)	Change in order of magnitude of CFUs with NO_3 amendments on ultrapure agarose plates	Change in order of magnitude of CFUs with NO_3 amendments on Luria-Bertani agar plates	Change in order of magnitude of CFUs with NO_3 amendments on plate count agar plates
0.7	52	0.38	-0.86	**-1.97**
1.1	160	-0.78	0.07	**-3.29**
2	16	**-1.17**	**-1.28**	**-3.38**
10	2.5	1.08	-0.23	-0.27
15	4500	-0.05	**-2.40**	-0.73
20	21	1.27	0.93	-0.25
30	82	0.64	0.33	-0.90

Author Contributions: J.S., A.Z. and M.C. sampled in the study sites. J.S. performed nitrate measurements under the supervision of M.C., TOC/TN determination under the supervision of E.S., soil characterization, cell culture, and all statistical analyses. E.S. interpreted XRF and TN data. All authors wrote and approved the final manuscript. Data curation, Jianxun Shen; Funding acquisition, Mark Claire; Investigation, Jianxun Shen; Methodology, Jianxun Shen and Eva Stueeken; Project administration, Aubrey Zerkle; Software, Jianxun Shen; Supervision, Aubrey Zerkle and Mark Claire; Validation, Aubrey Zerkle and Mark Claire; Visualization, Jianxun Shen; Writing – original draft, Jianxun Shen; Writing – review & editing, Aubrey Zerkle, Mark Claire and Eva Stueeken.

Funding: This research was funded by European Research Council (ERC) under the European Union's Horizon 2020 Research and Innovation Programme (Grant Agreement 678812) (to M.W.C.). J.S. also acknowledges support from the China Scholarship Council (CSC).

Acknowledgments: We thank S. Fischer for assisting the XRF analyses.

Conflicts of Interest: The authors declare no conflict of interest.

References

1. Franz, H.B.; Trainer, M.G.; Malespin, C.A.; Mahaffy, P.R.; Atreya, S.K.; Becker, R.H.; Benna, M.; Conrad, P.G.; Eigenbrode, J.L.; Freissinet, C., et al. Initial SAM calibration gas experiments on Mars: Quadrupole mass spectrometer results and implications. *Planet Space Sci* **2017**, *138*, 44-54, doi:10.1016/j.pss.2017.01.014.
2. Schuerger, A.C.; Mancinelli, R.L.; Kern, R.G.; Rothschild, L.J.; McKay, C.P. Survival of endospores of Bacillus subtilis on spacecraft surfaces under simulated martian environments: implications for the forward contamination of Mars. *Icarus* **2003**, *165*, 253-276.
3. Stern, J.C.; Sutter, B.; Freissinet, C.; Navarro-Gonzalez, R.; McKay, C.P.; Archer, P.D.; Buch, A.; Brunner, A.E.; Coll, P.; Eigenbrode, J.L., et al. Evidence for indigenous nitrogen in sedimentary and aeolian deposits from the Curiosity rover investigations at Gale crater, Mars. *P Natl Acad Sci USA* **2015**, *112*, 4245-4250, doi:10.1073/pnas.1420932112.
4. Navarro-Gonzalez, R.; Rainey, F.A.; Molina, P.; Bagaley, D.R.; Hollen, B.J.; de la Rosa, J.; Small, A.M.; Quinn, R.C.; Grunthaner, F.J.; Caceres, L., et al. Mars-like soils in the Atacama Desert, Chile, and the dry limit of microbial life. *Science* **2003**, *302*, 1018-1021, doi:DOI 10.1126/science.1089143.
5. Veblen, T.T.; Young, K.R.; Orme, A.R. *The physical geography of South America*; Oxford University Press: 2015.
6. McKay, C.P.; Friedmann, E.I.; Gomez-Silva, B.; Caceres-Villanueva, L.; Andersen, D.T.; Landheim, R. Temperature and moisture conditions for life in the extreme arid region of the Atacama Desert: Four years

of observations including the El Nino of 1997-1998. *Astrobiology* **2003**, *3*, 393-406, doi:Doi 10.1089/153110703769016460.

7. Hartley, A.J.; Chong, G.; Houston, J.; Mather, A.E. 150 million years of climatic stability: evidence from the Atacama Desert, northern Chile. *J Geol Soc London* **2005**, *162*, 421-424, doi:Doi 10.1144/0016-764904-071.
8. Houston, J. Variability of precipitation in the Atacama desert: Its causes and hydrological impact. *Int J Climatol* **2006**, *26*, 2181-2198, doi:10.1002/joc.1359.
9. Sun, T.; Bao, H.M.; Reich, M.; Hemming, S.R. More than ten million years of hyper-aridity recorded in the Atacama Gravels. *Geochim Cosmochim Ac* **2018**, *227*, 123-132, doi:10.1016/j.gca.2018.02.021.
10. Cordero, R.R.; Damiani, A.; Jorquera, J.; Sepulveda, E.; Caballero, M.; Fernandez, S.; Feron, S.; Llanillo, P.J.; Carrasco, J.; Laroze, D., et al. Ultraviolet radiation in the Atacama Desert. *Antonie Van Leeuwenhoek* **2018**, *111*, 1301-1313, doi:10.1007/s10482-018-1075-z.
11. Lester, Y.; Sharpless, C.M.; Mamane, H.; Linden, K.G. Production of Photo-oxidants by Dissolved Organic Matter During UV Water Treatment. *Environ Sci Technol* **2013**, *47*, 11726-11733, doi:10.1021/es402879x.
12. Quinn, R.C.; Ehrenfreund, P.; Grunthaner, F.J.; Taylor, C.L.; Zent, A.P. Decomposition of aqueous organic compounds in the Atacama Desert and in Martian soils. *J Geophys Res-Biogeo* **2007**, *112*, doi:Artn G04s18/10.1029/2006jg000312.
13. Michalski, G.; Bohlke, J.K.; Thiemens, M. Long term atmospheric deposition as the source of nitrate and other salts in the Atacama Desert, Chile: New evidence from mass-independent oxygen isotopic compositions. *Geochim Cosmochim Ac* **2004**, *68*, 4023-4038, doi:10.1016/j.gca.2004.04.009.
14. Kounaves, S.P.; Carrier, B.L.; O'Neil, G.D.; Stroble, S.T.; Claire, M.W. Evidence of martian perchlorate, chlorate, and nitrate in Mars meteorite EETA79001: Implications for oxidants and organics. *Icarus* **2014**, *229*, 206-213, doi:10.1016/j.icarus.2013.11.012.
15. Jaramillo, E.A.; Royle, S.H.; Claire, M.W.; Kounaves, S.P.; Sephton, M.A. Indigenous Organic-Oxidized Fluid Interactions in the Tissint Mars Meteorite. *Geophys Res Lett* **2019**, *46*, 3090-3098, doi:10.1029/2018gl081335.
16. Ewing, S.A.; Michalski, G.; Thiemens, M.; Quinn, R.C.; Macalady, J.L.; Kohl, S.; Wankel, S.D.; Kendall, C.; Mckay, C.P.; Amundson, R. Rainfall limit of the N cycle on Earth. *Global Biogeochem Cy* **2007**, *21*, doi:Artn Gb3009/10.1029/2006gb002838.
17. Azua-Bustos, A.; Fairen, A.G.; Gonzalez-Silva, C.; Ascaso, C.; Carrizo, D.; Fernandez-Martinez, M.A.; Fernandez-Sampedro, M.; Garcia-Descalzo, L.; Garcia-Villadangos, M.; Martin-Redondo, M.P., et al. Unprecedented rains decimate surface microbial communities in the hyperarid core of the Atacama Desert. *Sci Rep-Uk* **2018**, *8*, doi:ARTN 16706/10.1038/s41598-018-35051-w.
18. Bohlke, J.K.; Ericksen, G.E.; Revesz, K. Stable isotope evidence for an atmospheric origin of desert nitrate deposits in northern Chile and southern California, USA. *Chem Geol* **1997**, *136*, 135-152, doi:Doi 10.1016/S0009-2541(96)00124-6.
19. Catling, D.C.; Claire, M.W.; Zahnle, K.J.; Quinn, R.C.; Clark, B.C.; Hecht, M.H.; Kounaves, S. Atmospheric origins of perchlorate on Mars and in the Atacama. *J Geophys Res-Planet* **2010**, *115*, doi:Artn E00e11/10.1029/2009je003425.
20. Smith, M.L.; Claire, M.W.; Catling, D.C.; Zahnle, K.J. The formation of sulfate, nitrate and perchlorate salts in the martian atmosphere. *Icarus* **2014**, *231*, 51-64, doi:10.1016/j.icarus.2013.11.031.
21. Walvoord, M.A.; Phillips, F.M.; Stonestrom, D.A.; Evans, R.D.; Hartsough, P.C.; Newman, B.D.; Striegl, R.G. A reservoir of nitrate beneath desert soils. *Science* **2003**, *302*, 1021-1024, doi:DOI 10.1126/science.1086435.

22. Jackson, W.A.; Bohlke, J.K.; Andraski, B.J.; Fahlquist, L.; Bexfield, L.; Eckardt, F.D.; Gates, J.B.; Davila, A.F.; McKay, C.P.; Rao, B., et al. Global patterns and environmental controls of perchlorate and nitrate co-occurrence in arid and semi-arid environments. *Geochim Cosmochim Ac* **2015**, *164*, 502-522, doi:10.1016/j.gca.2015.05.016.
23. Hutchins, S.R. Biodegradation of Monoaromatic Hydrocarbons by Aquifer Microorganisms Using Oxygen, Nitrate, or Nitrous-Oxide as the Terminal Electron-Acceptor. *Appl Environ Microb* **1991**, *57*, 2403-2407.
24. Shapleigh, J.P. Dissimilatory and assimilatory nitrate reduction in the purple photosynthetic bacteria. In *The purple phototrophic bacteria*, Springer: 2009; pp. 623-642.
25. van de Graaf, A.A.; Mulder, A.; de Bruijn, P.; Jetten, M.S.; Robertson, L.A.; Kuenen, J.G. Anaerobic oxidation of ammonium is a biologically mediated process. *Appl Environ Microbiol* **1995**, *61*, 1246-1251.
26. Connon, S.A.; Lester, E.D.; Shafaat, H.S.; Obenhuber, D.C.; Ponce, A. Bacterial diversity in hyperarid Atacama Desert soils. *J Geophys Res-Biogeo* **2007**, *112*, doi:Artn G04s17/10.1029/2006jg000311.
27. Bagaley, D.R. Uncovering bacterial diversity on and below the surface of a hyper-arid environment, the Atacama Desert, Chile. Louisiana State University and Agricultural and Mechanical College, 2006.
28. Shirey, T.B. Investigating microbial communities and the environmental factors influencing them in manmade and naturally occurring systems. University of Alabama, Tuscaloosa, Alabama, 2013.
29. Neilson, J.W.; Califf, K.; Cardona, C.; Copeland, A.; van Treuren, W.; Josephson, K.L.; Knight, R.; Gilbert, J.A.; Quade, J.; Caporaso, J.G., et al. Significant Impacts of Increasing Aridity on the Arid Soil Microbiome. *Msystems* **2017**, *2*, doi:UNSP e00195-16/10.1128/mSystems.00195-16.
30. Crits-Christoph, A.; Robinson, C.K.; Barnum, T.; Fricke, W.F.; Davila, A.F.; Jedynak, B.; McKay, C.P.; DiRuggiero, J. Colonization patterns of soil microbial communities in the Atacama Desert. *Microbiome* **2013**, *1*, doi:Artn 28/10.1186/2049-2618-1-28.
31. Neilson, J.W.; Quade, J.; Ortiz, M.; Nelson, W.M.; Legatzki, A.; Tian, F.; LaComb, M.; Betancourt, J.L.; Wing, R.A.; Soderlund, C.A., et al. Life at the hyperarid margin: novel bacterial diversity in arid soils of the Atacama Desert, Chile. *Extremophiles* **2012**, *16*, 553-566, doi:10.1007/s00792-012-0454-z.
32. Drees, K.P.; Neilson, J.W.; Betancourt, J.L.; Quade, J.; Henderson, D.A.; Pryor, B.M.; Maier, R.M. Bacterial community structure in the hyperarid core of the Atacama Desert, Chile. *Appl Environ Microb* **2006**, *72*, 7902-7908, doi:10.1128/Aem.01305-06.
33. Lester, E.D.; Satomi, M.; Ponce, A. Microflora of extreme arid Atacama Desert soils. *Soil Biol Biochem* **2007**, *39*, 704-708, doi:10.1016/j.soilbio.2006.09.020.
34. Warren-Rhodes, K.A.; Rhodes, K.L.; Pointing, S.B.; Ewing, S.A.; Lacap, D.C.; Gomez-Silva, B.; Amundson, R.; Friedmann, E.I.; McKay, C.P. Hypolithic cyanobacteria, dry limit of photosynthesis, and microbial ecology in the hyperarid Atacama Desert. *Microb Ecol* **2006**, *52*, 389-398, doi:10.1007/s00248-006-9055-7.
35. Azua-Bustos, A.; Gonzalez-Silva, C.; Mancilla, R.A.; Salas, L.; Gomez-Silva, B.; McKay, C.P.; Vicuna, R. Hypolithic Cyanobacteria Supported Mainly by Fog in the Coastal Range of the Atacama Desert. *Microb Ecol* **2011**, *61*, 568-581, doi:10.1007/s00248-010-9784-5.
36. Lacap, D.C.; Warren-Rhodes, K.A.; McKay, C.P.; Pointing, S.B. Cyanobacteria and chloroflexi-dominated hypolithic colonization of quartz at the hyper-arid core of the Atacama Desert, Chile. *Extremophiles* **2011**, *15*, 31-38, doi:10.1007/s00792-010-0334-3.
37. Wierzchos, J.; Ascaso, C.; McKay, C.P. Endolithic cyanobacteria in halite rocks from the hyperarid core of the Atacama Desert. *Astrobiology* **2006**, *6*, 415-422, doi:DOI 10.1089/ast.2006.6.415.

38. Dong, H.L.; Rech, J.A.; Jiang, H.C.; Sun, H.; Buck, B.J. Endolithic cyanobacteria in soil gypsum: Occurrences in Atacama (Chile), Mojave (United States), and Al-Jafr Basin (Jordan) deserts. *J Geophys Res-Biogeo* **2007**, *112*, doi:Artn G02030/10.1029/2006jg000385.
39. Schulze-Makuch, D.; Wagner, D.; Kounaves, S.P.; Mangelsdorf, K.; Devine, K.G.; de Vera, J.P.; Schmitt-Kopplin, P.; Grossart, H.P.; Parro, V.; Kaupenjohann, M., et al. Transitory microbial habitat in the hyperarid Atacama Desert. *P Natl Acad Sci USA* **2018**, *115*, 2670-2675, doi:10.1073/pnas.1714341115.
40. Kanehisa, M.; Goto, S. KEGG: Kyoto Encyclopedia of Genes and Genomes. *Nucleic Acids Res* **2000**, *28*, 27-30, doi:DOI 10.1093/nar/28.1.27.
41. Glass, C.; Silverstein, J. Denitrification of high-nitrate, high-salinity wastewater. *Water Res* **1999**, *33*, 223-229, doi:Doi 10.1016/S0043-1354(98)00177-8.
42. Ewing, S.A.; Macalady, J.L.; Warren-Rhodes, K.; McKay, C.P.; Amundson, R. Changes in the soil C cycle at the arid-hyperarid transition in the Atacama Desert. *J Geophys Res-Biogeo* **2008**, *113*, doi:Artn G02s90/10.1029/2007jg000495.
43. Jones, D.L.; Olivera-Ardid, S.; Klumpp, E.; Knief, C.; Huil, P.W.; Lehndorff, E.; Bol, R. Moisture activation and carbon use efficiency of soil microbial communities along an aridity gradient in the Atacama Desert. *Soil Biol Biochem* **2018**, *117*, 68-71, doi:10.1016/j.soilbio.2017.10.026.
44. Azua-Bustos, A.; Gonzalez-Silva, C.; Arenas-Fajardo, C.; Vicuna, R. Extreme environments as potential drivers of convergent evolution by exaptation: the Atacama Desert Coastal Range case. *Front Microbiol* **2012**, *3*, doi:ARTN 426/10.3389/fmicb.2012.00426.
45. Azua-Bustos, A.; Gonzalez-Silva, C.; Mancilla, R.A.; Salas, L.; Palma, R.E.; Wynne, J.J.; McKay, C.P.; Vicuna, R. Ancient Photosynthetic Eukaryote Biofilms in an Atacama Desert Coastal Cave. *Microb Ecol* **2009**, *58*, 485-496, doi:10.1007/s00248-009-9500-5.
46. Paulino-Lima, I.G.; Azua-Bustos, A.; Vicuna, R.; Gonzalez-Silva, C.; Salas, L.; Teixeira, L.; Rosado, A.; Leitao, A.A.D.; Lage, C. Isolation of UVC-Tolerant Bacteria from the Hyperarid Atacama Desert, Chile. *Microb Ecol* **2013**, *65*, 325-335, doi:10.1007/s00248-012-0121-z.
47. Paulino-Lima, I.G.; Fujishima, K.; Navarrete, J.U.; Galante, D.; Rodrigues, F.; Azua-Bustos, A.; Rothschild, L.J. Extremely high UV-C radiation resistant microorganisms from desert environments with different manganese concentrations. *J Photoch Photobio B* **2016**, *163*, 327-336, doi:10.1016/j.jphotobiol.2016.08.017.
48. Azua-Bustos, A.; Gonzalez-Silva, C.; Corsini, G. The Hyperarid Core of the Atacama Desert, an Extremely Dry and Carbon Deprived Habitat of Potential Interest for the Field of Carbon Science. *Front Microbiol* **2017**, *8*, doi:ARTN 993/10.3389/fmicb.2017.00993.
49. Canfield, D.E.; Glazer, A.N.; Falkowski, P.G. The evolution and future of Earth's nitrogen cycle. *Science* **2010**, *330*, 192-196, doi:10.1126/science.1186120.
50. Devol, A.H. Nitrogen cycle: Solution to a marine mystery. *Nature* **2003**, *422*, 575-576, doi:10.1038/422575a.
51. Jochum, K.P.; Nohl, L.; Herwig, K.; Lammel, E.; Stoll, B.; Hofmann, A.W. GeoReM: A new geochemical database for reference materials and isotopic standards. *Geostand Geoanal Res* **2005**, *29*, 333-338, doi:DOI 10.1111/j.1751-908X.2005.tb00904.x.
52. *Origin(Pro)*, 2018; OriginLab Corporation: Northampton, MA, USA.
53. *IBM SPSS Statistics for Windows*, 25.0; IBM Corp.: Armonk, NY, 2017.
54. Duncan, O.D. Path Analysis - Sociological Examples. *Am J Sociol* **1966**, *72*, 1-16, doi:Doi 10.1086/224256.
55. Shipley, B. *Cause and correlation in biology: a user's guide to path analysis, structural equations and causal inference with R*; Cambridge University Press: 2016.

56. Block, G.A.; Pergola, P.E.; Fishbane, S.; Martins, J.G.; LeWinter, R.D.; Uhlig, K.; Neylan, J.F.; Chertow, G.M. Effect of ferric citrate on serum phosphate and fibroblast growth factor 23 among patients with nondialysis-dependent chronic kidney disease: path analyses. *Nephrol Dial Transplant* **2019**, *34*, 1115-1124, doi:10.1093/ndt/gfy318.
57. Loehlin, J.C. Latent Variable Models - an Introduction to Factor, Path, and Structural-Analysis - Loehlin,Jc. *Appl Psych Meas* **1988**, *12*, 211-213.
58. Arbuckle, J.L. *Amos*, 25.0; IBM SPSS: Chicago, 2017.
59. Wierzchos, J.; Camara, B.; De Los Rios, A.; Davila, A.F.; Almazo, I.M.S.; Artieda, O.; Wierzchos, K.; Gomez-Silva, B.; Mckay, C.; Ascaso, C. Microbial colonization of Ca-sulfate crusts in the hyperarid core of the Atacama Desert: implications for the search for life on Mars. *Geobiology* **2011**, *9*, 44-60, doi:10.1111/j.1472-4669.2010.00254.x.
60. Parro, V.; de Diego-Castilla, G.; Moreno-Paz, M.; Blanco, Y.; Cruz-Gil, P.; Rodriguez-Manfredi, J.A.; Fernandez-Remolar, D.; Gomez, F.; Gomez, M.J.; Rivas, L.A., et al. A Microbial Oasis in the Hypersaline Atacama Subsurface Discovered by a Life Detector Chip: Implications for the Search for Life on Mars. *Astrobiology* **2011**, *11*, 969-996, doi:10.1089/ast.2011.0654.
61. Oberlin, E.A.; Claire, M.W.; Kounaves, S.P. Evaluation of the Tindouf Basin Region in Southern Morocco as an Analog Site for Soil Geochemistry on Noachian Mars. *Astrobiology* **2018**, *18*, 1318-1328, doi:10.1089/ast.2016.1557.
62. Schroeder, P.A.; McLain, A.A. Illite-smectites and the influence of burial diagenesis on the geochemical cycling of nitrogen. *Clay Miner* **1998**, *33*, 539-546, doi:Doi 10.1180/000985598545877.
63. Bebout, G.E.; Fogel, M.L. Nitrogen-Isotope Compositions of Metasedimentary Rocks in the Catalina Schist, California - Implications for Metamorphic Devolatilization History. *Geochim Cosmochim Ac* **1992**, *56*, 2839-2849, doi:Doi 10.1016/0016-7037(92)90363-N.
64. Farmer, J.D.; Des Marais, D.J. Exploring for a record of ancient Martian life. *J Geophys Res-Planet* **1999**, *104*, 26977-26995, doi:Doi 10.1029/1998je000540.
65. Hays, L.E.; Graham, H.V.; Marais, D.J.D.; Hausrath, E.M.; Horgan, B.; McCollom, T.M.; Parenteau, M.N.; Potter-McIntyre, S.L.; Williams, A.J.; Lynch, K.L. Biosignature Preservation and Detection in Mars Analog Environments. *Astrobiology* **2017**, *17*, 363-+, doi:10.1089/ast.2016.1627.
66. Dong, H.L. Clay-Microbe Interactions and Implications for Environmental Mitigation. *Elements* **2012**, *8*, 113-118, doi:10.2113/gselements.8.2.113.
67. Ogur, R.; Coskun, O.; Korkmaz, A.; Oter, S.; Yaren, H.; Hasde, M. High nitrate intake impairs liver functions and morphology in rats; protective effects of alpha-tocopherol. *Environ Toxicol Phar* **2005**, *20*, 161-166, doi:10.1016/j.etap.2004.12.051.
68. Romano, N.; Zeng, C. Acute toxicity of sodium nitrate, potassium nitrate, and potassium chloride and their effects on the hemolymph composition and gill structure of early juvenile blue swimmer crabs (Portunus pelagicus Linnaeus, 1758) (Decapoda, Brachyura, Portunidae). *Environ Toxicol Chem* **2007**, *26*, 1955-1962, doi:Doi 10.1897/07-144r.1.
69. Romano, N.; Zeng, C. Effects of potassium on nitrate mediated alterations of osmoregulation in marine crabs. *Aquat Toxicol* **2007**, *85*, 202-208, doi:10.1016/j.aquatox.2007.09.004.
70. Carr, M.H.; Head, J.W. Geologic history of Mars. *Earth Planet Sc Lett* **2010**, *294*, 185-203, doi:10.1016/j.epsl.2009.06.042.

71. Fuller, E.R.; Head, J.W. Amazonis Planitia: The role of geologically recent volcanism and sedimentation in the formation of the smoothest plains on Mars. *J Geophys Res-Planet* **2002**, *107*, doi:Artn 5081/10.1029/2002je001842.
72. Clifford, S.M.; Parker, T.J. The evolution of the Martian hydrosphere: Implications for the fate of a primordial ocean and the current state of the northern plains. *Icarus* **2001**, *154*, 40-79, doi:10.1006/icar.2001.6671.
73. Di Achille, G.; Hynek, B.M. Ancient ocean on Mars supported by global distribution of deltas and valleys. *Nat Geosci* **2010**, *3*, 459-463, doi:10.1038/Ngeo891.
74. Malin, M.C.; Edgett, K.S. Evidence for persistent flow and aqueous sedimentation on early Mars. *Science* **2003**, *302*, 1931-1934, doi:10.1126/science.1090544.
75. Irwin, R.P.; Maxwell, T.A.; Howard, A.D.; Craddock, R.A.; Leverington, D.W. A large paleolake basin at the head of Ma'adim Vallis, Mars. *Science* **2002**, *296*, 2209-2212, doi:DOI 10.1126/science.1071143.
76. Craddock, R.A.; Howard, A.D. The case for rainfall on a warm, wet early Mars. *J Geophys Res-Planet* **2002**, *107*, doi:Artn 5111/10.1029/2001je001505.
77. Gómez-Silva, B.; Rainey, F.A.; Warren-Rhodes, K.A.; McKay, C.P.; Navarro-González, R. Atacama Desert soil microbiology. In *Microbiology of extreme soils*, Springer: Berlin, Heidelberg, 2008; pp. 117-132.